Food Hydrocolloids 137 (2023) 108364

Contents lists available at ScienceDirect

Food Hydrocolloids

journal homepage: www.elsevier.com/locate/foodhyd

Effect of molecular structure changes during starch gelatinization on its rheological and 3D printing properties

Yue Cheng [a,b,c], Kexin Liang [b,c], Yifan Chen [b,c], Wei Gao [b,c], Xuemin Kang [a,b,c], Tianze Li [b,c], Bo Cui [a,b,c,*]

[a] Department of Food Science and Engineering, Shandong Agricultural University, Taian, 271018, China
[b] State Key Laboratory of Biobased Material and Green Papermaking, Qilu University of Technology, Shandong Academy of Sciences, Jinan, 250353, China
[c] School of Food Science and Engineering, Qilu University of Technology, Shandong Academy of Sciences, Jinan, Shandong, 250353, China

ARTICLE INFO

Keywords:
Starch
3D printing
Rheological properties
Treating temperatures
Linear chain length distributions

ABSTRACT

Although the changes in molecular structure during starch gelatinization has been intensively investigated, how a relationship between starch rheological properties, printability, and starch molecular structure changes during starch gelatinization remains unclear. This research is focused on the molecular structure changes of corn starch (CS) gels caused by different treatment temperatures and their effects on CS gel rheological and 3D printing properties. With increasing treatment temperature, the leached amylose content and short linear chains (DP 6–12) of CS increase, whereas the contents of long linear chains (DP > 12) decrease, which influences the rheological and 3D printing properties of starch. Due to the presence of the original granules and crystalline structure, the CS-65 starch gel presented a poor storage modulus (G′), indicating poor 3D printing performance. The leaching of amylose induced the formation of new crystal and cross-linked network structures, which is beneficial for increasing its G′. However, the increase in short amylopectin linear chains (DP 6–12) reduced the degree of short-range order and hydrogen bonding interactions, which was detrimental to its G′ and yield stress (τf). CS-80 starch gel exhibited the largest G′ and shear recovery rate, showing the highest self-supporting properties and printing precision. Extremely high temperatures contributed to the densification of the starch gel structure, which led to an increase in τf and difficult extrusion. Overall, molecular structural changes caused by starch gelatinization are critical to its ideal rheological properties for 3D printing.

1. Introduction

3D printing technology is a technology based on computer digital technology, through three-dimensional modeling, model slicing, information processing, layer-by-layer printing and other steps to finally form a three-dimensional entity technology, which integrates digital processing technology, computer technology, numerical control technology, material technology and many other modern technologies (Chen, Zhang, Sun, & Phuhongsung, 2021). 3D printing technology can quickly and accurately convert the designer's product design into physical components (Dankar, Haddarah, Omar, Sepulcre, & Pujolà, 2018). It has many advantages in the food industry such as customized design of food structure, personalized and digital nutrition customization, simplified supply chain, and broadened sources of food raw materials. Therefore, applying 3D printing to the food industry will produce a technological revolution.

Extrusion 3D printing creates solids by extruding material from a nozzle, layer by layer. First, the printed material must have good flow properties for easy extrusion from the nozzle, and second, it needs to have suitable viscoelasticity to form continuous lines after extrusion from the nozzle for deposition molding (Godoi, Prakash, & Bhandari, 2016). Therefore, in the 3D printing process, because the material will experience high shear when it is extruded from the nozzle, it is necessary for the material to have suitable yield stress (τf) to facilitate extrusion flow. Meanwhile, it needs to have a lower viscosity during the process of passing through the nozzle, which is conducive to smooth extrusion. Therefore, the printing material is required to have the characteristics of shear thinning. On the other hand, after the material is extruded from the nozzle, it needs quickly attain a certain structural strength to support subsequent deposition molding (Cui, Li, Guo, Liu, & Yang, 2021a,

* Corresponding author. Qilu University of Technology, (Shandong Academy of Sciences), Daxue Road, Changqing District, Jinan, Shandong Province, 250353, China.
E-mail address: cuibopaper@163.com (B. Cui).

https://doi.org/10.1016/j.foodhyd.2022.108364
Received 14 October 2022; Received in revised form 22 November 2022; Accepted 24 November 2022
Available online 28 November 2022
0268-005X/© 2022 Published by Elsevier Ltd.

2021b). Specifically, the printed material needs to have a fast and reversible modulus response to shear stress to ensure the high resolution of the printed body and to have a certain structural strength to prevent the printed body from collapsing and deforming. It can be concluded that the evolution of the rheological behavior of the printing material during the printing process plays a key role in extrusion 3D printing molding.

As a natural polymer material, starch is a typical pseudoplastic non-Newtonian fluid with shear thinning and thixotropy. This rheological property gives starch potential for 3D printing ink materials (Zhang et al., 2022). Moreover, starch is the main component in cereal food, and its rheological properties play a key role in the rheological properties of the cereal food material system, which provides the possibility for extrusion 3D printing technology to be applied to the manufacture of nutritious and healthy cereal food (Zhang et al., 2022). Starch gelatinization occurs during the processing of starch-based 3D-printing materials, contributing to their unique physicochemical properties. Starch gelatinization is the entry of water molecules into starch granules, which destroys the hydrogen bonds between starch molecules and makes starch molecules dispersed in water to become colloidal solution (Wang et al., 2021). The gelatinization process of starch involves changes in its structural changes, which will significantly affect the rheological properties of starch (Ai & Jane, 2015). For example, shorter A and B1 chains of starch lead to wheat flour paste having more elastic behavior, while a higher content of A and B1 chains leads to more viscous behavior (Zhang et al., 2020). Ji et al. (2022) also reported that the content of short amylopectin chains (DP 13–24) had a significant negative correlation with the consistency of starch, which was beneficial to the 3D printing process. Zeng, Chen, Chen, and Zheng (2021) also reported that the storage modulus and τf of starch gel were associated with the change in crystal structure during starch gelatinization, which significantly affects its extrusion process and self-supporting properties during 3D printing. It is clear that the molecular structure, especially the starch chain structure, significantly affected the rheological properties of the starch material. Previous studies have mainly focused on the changes in molecular structure during starch gelatinization (Wang et al., 2021), but lacking information about the changes in starch chain structure. Meanwhile, the causes of different starch rheological properties and printability during starch gelatinization, and whether these differences are related to the starch molecular structure changes, especially changes in starch chain structure, remain unknown.

In this study, through an experimental method of heating corn starch (CS) at different temperatures (65, 70, 80, 90, 100 °C), we tested various corn starch samples to reveal the structural changes, especially chain-length distributions (CLDs) of debranched starch, of corn starch during gelatinization. We mainly describe the relationship between starch molecular structure changes during starch gelatinization and its rheological properties and printing properties from the perspective of starch chain structure. These results will provide new insights into the theoretical basis for rheological properties of starch-based materials based on gelatinization of starch.

2. Materials and methods

2.1. Materials

Commercial corn starch was provided by COFCO Corporation (Beijing, China). Amylose content in starch was 33.81%, determined through an amylose content assay kit (BC4260, Beijing Solarbio Science & Technology Co., Ltd., Beijing, China). Dimethyl sulfoxide (chromatographic purity), sodium nitrate, dimethyl sulfoxide-D6, sodium acetate ≥99.0% and glacial acetic acid were acquired from Sigma Co., Ltd. (St. Louis, MO, USA). Isoamylase was secured from Shanghai Anpu Experimental Technology Co., Ltd. (Shanghai, China).

2.2. Sample preparation

Weigh a certain amount of corn starch (CS) and add distilled water to make a 20% suspension. Then, place the mixture into a water bath at 65, 70, 80, 90, and 100 °C and stir evenly for 15 min at 600 rpm/min. The mixture was injected into the printer syringe after cooling to room temperature (20–25 °C) and kept in the refrigerator overnight at 4 °C (24 h in total). Starch samples treated at 65, 70, 80, 90 and 100 °C were coded as CS-65, CS-70, CS-80, CS-90 and CS-100, respectively.

2.3. Chain length distribution (CLDs) of amylopectin

Starch CLDs were characterized by a previous method (Tang et al., 2022). First, the starch gel samples were debranched. The specific method was as follows: 9 mg of starch was accurately weighed, dissolved in 450 μL of 100% DMSO, and stirred overnight. Then, 2250 μL of ultrapure water and 300 μL of pH 4.5 M sodium acetate buffer solution were added to dilute the starch solution. Finally, 1 μL of isoamylase was added. The debranching reaction was performed under continuous stirring for 12 h at room temperature, and the reaction was terminated by heating in a boiling water bath. The debranched sample solution was centrifuged and passed through a 0.45 μm filter membrane before being injected into the HPLC system.

The chain length distribution of the samples was determined by high-performance anion exchange chromatography (DIONEX ICS-5000+, Thermo Fisher Inc., USA.) with pulsed amperometric detection. After the sample was injected into the system, it was eluted with 150 mM sodium hydroxide solution (eluent A) and 150 mM sodium hydroxide containing 500 mM sodium acetate solution (eluent B) at a flow rate of 1 mL/min.

2.4. Leached amylose content

The amylose content of starch was determined according to a previous report (Yin et al., 2021). The leaching of corn starch samples was determined using a METASH UV-6100 spectrophotometer (Shanghai Yuanjie Instrument Co., Ltd., Shanghai, China). Technical support is provided by Sanshu Biotech. Co., LTD (Shanghai, China). The corn starch was heated to 65, 70, 80, 90 and 100 °C for 15 min at 600 rpm/min. Then, starch gel samples were cooled to room temperature and KI-I_2 reagent were added. Standard blank samples were used as controls, and samples were measured at 620 nm. A standard curve was determined, and the apparent amylose content was calculated from the standard curve.

2.5. Scanning electron microscopy (SEM)

The starch gel after freezing was used for SEM testing. After affixing a layer of conductive double-sided tape on the sample stage, the starch sample was pasted on the double-sided tape and then placed in an ion sputtering coater for gold plating for a certain period of time. Then, the samples were placed into a scanning electron microscope sample chamber and tested in the high voltage mode of 20 kV, and their cross-sectional morphology was observed at a magnification of 500 × by scanning electron microscopy (SEM, Hitachi SU3500, Tokyo, Japan).

2.6. Rapid viscosity analysis of potato starch

In order to obtain the information of starch gelatinization, 2.5 g corn starch (dry basis) and water was weighed to a total weight of 28 g and transferred to the aluminium cylinder of a rapid viscosity analyser (RVA TecMaster, Perten Instruments, Inc., Hagersten, Sweden). The suspension was stirred with matching propellers at the standard I program. The detail program condition was as follows: the suspension was held at 50 °C for l min and heated to 95 °C at a rate of 12 °C/min and held at 95 °C for 5 min. The paste was cooled down at a rate of 12 °C/min to

50 °C and held at 50 °C for 2 min.

2.7. X-ray diffraction (XRD)

The crystal structure of starch gels after freezing was measured using a D8 Advance X-ray diffractometer (Bruker–AXS, Karlsruhe, Germany) with a diffraction angle (2θ) ranging from 5° to 40° at a scanning rate of 0.02°/s at room temperature. All obtained curve were normalized for comparison.

2.8. Fourier transform infrared spectroscopy (FTIR)

FTIR was used to assess the lyophilised powder of the starch gel samples with different treatment temperatures obtained in section 2.2. Powder (2 mg) was combined with 100 mg of KBr before being pressed into tablets for measurement. The FTIR (Bruker, V70FTIR, Berlin, Germany) machine carried out 16 scans and recorded the spectrum at a speed of 0.16 cm^{-1} in the wavelength range of 4000–350 cm^{-1}. The molecular interaction between corn starch at various temperatures was explored in detail through Peak Fit, and the infrared absorbance at 995/1022 cm^{-1} (DD) was mainly studied. All spectra were baseline adjusted and normalized.

2.9. Rheological measurements

The rheological properties of the gel system were measured by MCR 102 modular intelligent rheometer (Anton Paar, Austria) with a plate diameter of 40 mm and a test spacing of 100 μm. In the static rheological test, the shear rate was set from 0.01 to 100 s^{-1}, and the η and stress of the samples were measured at 25 °C. In the stress sweep test, the stress was 1–1000 Pa or the upper stress limit of the rheometer, and the τf of the gel system was determined at 25 °C. τf is defined as the stress value when G′ and G″ are equal. When measuring the shear recovery characteristics of the gel system, the temperature was set at 25 °C, and shearing was performed at a low shear rate of 1 s^{-1} for 180 s, followed by continuous shearing at a high shear rate of 100 s^{-1} for 120 s and final shear at a low shear rate of 1 s^{-1} for 180 s. The shear recovery characteristics of the system were characterized by the ratio of the η value of the system in the first 30 s of the third stage to the average η of the first stage. In addition, the dynamic rheological measurement conditions are 25 °C, the strain is 0.1%, and the angular frequency is 0.1–100 rad/s. All tests were performed in the linear viscoelastic region of the sample.

2.10. 3D printing

A SHINNOVE-S2 printer was used for 3D printing (Shiyin Tech Co., Ltd., Hangzhou, China). The print 3D model was a cuboid with 20 mm height, 40 mm width and 40 mm length. The gel system was slowly added to the syringe without introducing air bubbles. According to the pre-experimental results, the setup parameters of the 3D printer were as follows: 24 mm/s printing rate, 0.84 mm nozzle diameter, and 25 °C extrusion temperature. The polymer fluid extrudes and swells during the extrusion process, which directly affects the width of the filament and the accuracy of the printed line. Therefore, it can be used to characterize the accuracy of the printed line. The smaller is the filament width, the higher is the resolution of the printed object.

The number of layers refers to the maximum number of layers that can be printed without the material being collapsed and deformed. The more layers the material has, the more suitable is the material for 3D printing. First, a pre-extrusion step was performed to eliminate nozzle clogging. The model was selected to print a cylindrical thin wall with a thickness of 32 × 32 × 40 mm, and the printing layer height was 0.7 mm. The obtained results were used to determine the number of printing layers. Set the relative height of the nozzle to 1.0 mm, the printing speed to 24 mm/s, the retraction speed to 50 mm/s, the retraction distance to 2 mm, and the inner diameter of the nozzle to 0.84 mm. The highest number of printing layers was tested three times, and the average value was calculated.

2.11. Statistical analysis

SPSS (Version 26.0, IBM Inc., USA) software was used to test the statistical significance of the data, expressed as x ± s. The comparison between the two groups of data was performed by one-way analysis of variance, and $P < 0.05$ was considered statistically significant.

3. Results and discussion

3.1. Chain length distributions of amylopectin and apparent amylose content

The chain length distribution of amylopectin can be divided into four parts according to the degree of polymerization (DP), including the A (DP 6–12), B_1 (DP 13–24), B_2 (DP 25–36) and B_3 (DP > 36) chains (Madhusudhan & Tharanathan, 1996). The outermost A chain of amylopectin is the shortest and connects the reducing end to other chains through α-1,6 bonds (Hanashiro et al., 1996). In addition, researchers have also reported that shorter amylopectin chains (A and B_1) are the main cause of double helix formation in starch granules, which involves the formation of crystalline regions in starch granules (Li et al., 2020). As shown in Table 1, the contents of A-chain and leached amylose both increased with increasing treatment temperature, while the content of B_1-chains, as the main type of amylopectin branch, decreased. The contents of B_2-chains first increased and then decreased when the treatment temperature increased from 65 to 100 °C. With increasing temperature from 65 to 70 °C, the contents of B_2 and B_3-chains also decreased, while B_3-chains did not show a significant change when the treatment temperature increased from 70 to 100 °C. These results indicate that high temperature destroys the medium and long chains of amylopectin (DP > 12) in the initial stage of gelatinization, breaking it down into short chains (DP 6–12). As starch gelatinization continues, the energy absorbed at high temperature mainly destroys the lateral chains (DP 13–36) of amylopectin. Wang, Li, Liu, & Zheng (2022) also used physical method (heat-moisture treatment) to modify starch, which had less damage to starch amylopectin and only slightly affected the proportion of A-chains. Compared with physical modification, chemical modification (acid treatment) and biological modification (pullulanase treatment) are more efficient ways to change the distribution of amylopectin chain length, but they also depend on the concentration of modified reagent and reaction time (Li & Hu, 2021; Tang et al., 2022). On the other hand, more amylose leaches out due to the breakdown of the amylopectin structure. The leached amylose may adhere to the amylopectin to prevent the thermal energy from damaging it, thus leading to the increase of B_2-chains content with the increasing

Table 1
Amylopectin chain length distribution and amylopectin content of corn starch gels treated at different temperatures.

Sample	A-chains (%)(DP 6–12)	B_1-chains (%)(DP 13–24)	B_2-chains (%)(DP 25–36)	B_3-chains (%)(DP > 36)	Apparent amylose content (%)
CS-65	31.91 ± 0.11e	51.05 ± 0.02a	12.32 ± 0.03a	4.75 ± 0.12a	6.13 ± 0.12e
CS-70	34.53 ± 0.02d	50.42 ± 0.14b	11.16 ± 0.32b	3.99 ± 0.16b	10.14 ± 0.41d
CS-80	35.34 ± 0.07c	49.87 ± 0.05c	10.79 ± 0.04c	4.02 ± 0.15b	16.12 ± 0.21c
CS-90	36.34 ± 0.13b	48.31 ± 0.07d	11.25 ± 0.07b	4.03 ± 0.02b	22.54 ± 0.13b
CS-100	38.72 ± 0.05a	47.06 ± 0.14e	11.29 ± 0.11b	4.01 ± 0.11b	26.12 ± 0.11a

Different lowercase letters within the same column indicate significant differences among the samples ($p < 0.05$).

temperature from 80 to 100 °C.

3.2. Morphology

As shown in Fig. 1, the microscopic morphology of starch gel samples was observed by scanning electron microscopy. When the heating temperature is 62 °C, the starch begins to gelatinize (Fig. S1), and the starch granules slightly swelled and absorbed a small amount of water. Therefore, as shown in Fig. 1a, the corn starch treated at 65 °C shows an expanded granular structure, while not well-cross-linked together, indicating a lower gelatinization degree. With increasing treatment temperature, the starch granules further absorb water, swell and gradually rupture (Fig. 1(b–e)). When the temperature increased to 80 °C, the starch granule structure basically disappeared, and the system formed a cluster structure that resembled coral clumps, indicating that higher temperatures promote starch gelatinization and the formation of a cross-linked network structure. With a further increase in the starch treatment temperature, the clustered structure of the gel samples showed some cracks (as marked by the red circle) and small pieces, indicating that excessively high temperatures may have broken the structure of the starch gel. This result may be attributed to the high content of short chains (DP 6–12) in the samples at processing temperatures, which are less able to entangle and link with each other, resulting in lower stiffness and bonding ability (Liu, Chen, Bie, Xie, & Zheng, 2021). Moreover, the presence of cracks and small pieces may be related to the reduction of short-range molecular order (as proven by Section 3.4), which is closely related to matrix free volume or spacer junction regions (Huang, Chao, Yu, Copeland, & Wang, 2021).

3.3. Crystalline structure

To investigate the influence of the crystalline structure of starch gel, the printed starch samples was characterized by wide-angle X-ray diffraction, and the results are shown in Fig. 2. The CS-65 starch gel sample exhibited an A-type crystalline structure with diffraction at 17°, 18° and 23° and a B-type crystalline structure with diffraction peaks at 24° (Cheng, Gao, Wang, Hou, & Lim, 2022; Gao et al., 2021). As the processing temperature increased to 70 °C, the A-type crystallization peak of starch became weaker, while the V-type crystallization characteristic (diffraction peak at 19.8°) peak appeared. When the treatment temperatures were in the range of 80–90 °C, starch gel materials retained the characteristic diffraction peaks of the B-type crystalline structure (diffraction peak at 17.1°). Moreover, the diffraction peak intensity of 19.8° increased as the temperature increased, indicating a stronger V-type crystalline structure. The enhancement of the V-type crystalline structure was attributed to the leaching of amylose, which formed starch-lipid complexes with the endogenous starch lipids, manifesting as V-shaped crystals (Kang et al., 2020). The appearance of the B-type diffraction peak usually shows the formation of a double helix structure between amylose and amylopectin, indicating the degree of starch retrogradation (Huang et al., 2021). The formation of new starch crystal structures was helpful to improve the structural strength of starch gel systems (Zeng et al., 2021), such as the V-type structure and B-type crystalline structure in this study.

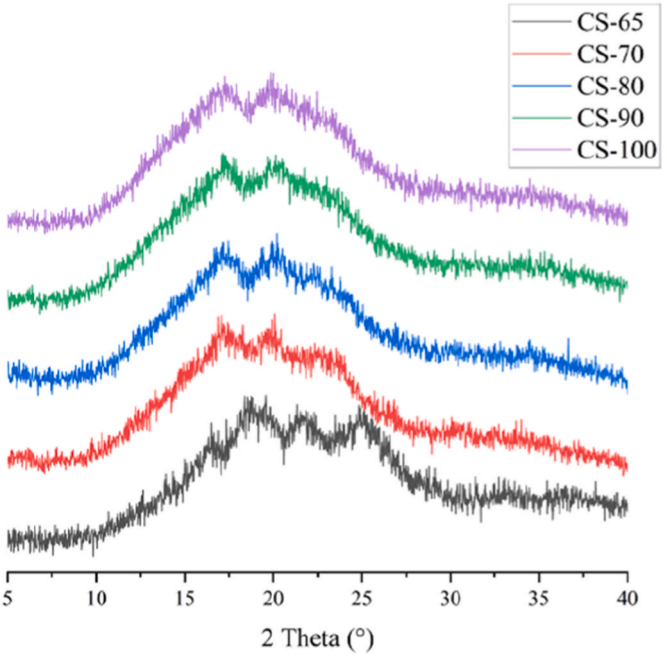

Fig. 2. X-ray diffraction of corn starch gels treated at different temperatures.

3.4. FTIR

The FTIR spectra of the heat-treated starch gels are shown in Fig. 3a. The broad band around 3423 cm^{-1} corresponds to the stretching vibration of the hydroxyl groups (Cheng et al., 2023). In the current study, this peak shifts toward lower wavenumbers when the treatment temperature increases from 65 to 90 °C, indicating the enhancement of hydrogen bonding. This may be due to the formation of new intermolecular hydrogen bonds caused by the leached amylose, which are greater in number than the disrupted intramolecular hydrogen bonds. When the treatment temperature increased from 90 °C to 100 °C, the hydroxyl peak shifted to higher wavenumbers, which may be attributed to the presence of more short starch chains (DP 6–12). This short-chain structure inhibits chain-to-chain interactions and hinders the formation of hydrogen bonds between starch molecules (Liu et al., 2021). The raw spectra were deconvolved in the 1100–900 cm^{-1} region to further investigate the effect of treatment temperature on the CS short-range structure, and the result is shown in Fig. 3b. The absorption band at 1022 cm^{-1} represents the relative content of starch amorphous structure, while the absorption band at 994 cm^{-1} is bound to the intramolecular hydrogen bonding of hydroxyl groups, promoting the degree of double helical order (short-range order). Therefore, the ratio of 995/1022 cm^{-1} can be used to determine changes in the short-range order of the starch gel system. Among all samples, the CS-65 starch gel has the highest ratio of 995/1022 cm^{-1}, which is because of the retention of more original crystal structures due to the lower degree of gelatinization, leading to its higher degree of short-range molecular order. With the increase in treatment temperature from 70 to 100 °C, a trend of increasing first and then decreasing in the ratio of 995/1022

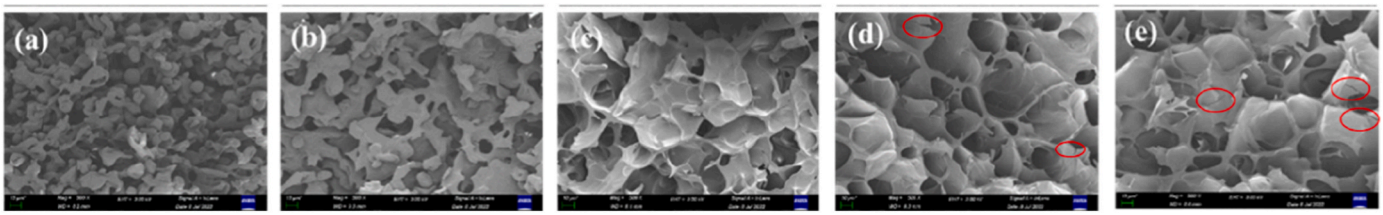

Fig. 1. SEM images of starch gels treated at different temperatures: (a) CS-65, (b) CS-70, (c) CS-80, (d) CS-90 and (e) CS-100.

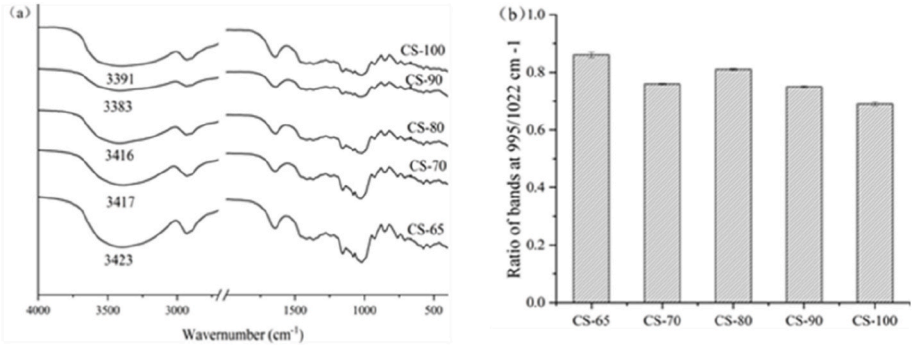

Fig. 3. FTIR spectra of corn starch treated at different temperatures.

cm^{-1} was observed, indicating that CS-80 starch gel sample showed a higher degree of short-range molecular order. Compared with CS-70 starch gel sample, the higher short-range molecular order of CS-80 starch gel sample could be attributed to the fact the increase of treatment temperature promoted the leach of amylose for an improved alignment, which promotes the formation of starch ordered structure (Lu et al., 2023). However, the increase of treatment temperature also leaded to the formation of starch short chains (DP 6–12), which might reduce the collision possibility of starch chains in a disordered state owing to gelatinization (Liu et al., 2021), thus inhibiting the formation of the ordered structure of starch during retrogradation.

3.5. Dynamic rheological measurements

3.5.1. Steady shear rheological study

In the extrusion 3D printing process, because the material experiences high shear when it is extruded through a very fine nozzle, it is necessary for the printing material to have the characteristics of shear thinning to facilitate smooth extrusion. The viscosity versus shear rate profile of different treatment temperatures of corn starch is shown in Fig. 4. The viscosity of all samples decreased with increasing shear rate and exhibited shear thinning characteristics, showing greater potential as a 3D printing material. The shear thinning phenomenon of macromolecular fluids, such as starch, can be explained by the orientation and alignment of chains under shear force. The CS-65 starch gel sample exhibits a stronger linear viscosity reduction, while the linear behavior of the other obtained samples was weaker. The network structure composed of cross-linking points is in a state of continuous construction and disintegration due to the external shear force; thus, it can be vividly called a "transient network". With increasing treatment temperature, the starch molecular chain was slowly opened, and hydrophilic groups (such as hydroxyl groups) were exposed, increasing the number of interaction sites for cooperative zipping to occur between aligned chains (Wee, Matia-Merino, & Goh, 2015). At lower shear rates, the starch gels treated at higher temperatures appeared to sufficiently stretch out with shear flow to allow some intermolecular associations between neighboring polymer chains to occur. The occurrence of this association and disaggregation phenomenon results in a weaker linear change in viscosity (Cai, Goh, Lim, & Matia-Merino, 2021).

At lower shear rates (0.1–10 s^{-1}), the viscosity of starch gel increased with increasing treatment temperature. This was attributed to the fact that high temperature promotes gelatinization of starch, which promotes the disintegration of the starch double helix structu re, and the molecular chain is fully stretched to form a new chain entanglement or hydrogen bond, increasing the resistance during shearing (Wang et al., 2021; Zeng et al., 2021). However, the viscosity of the CS-80 starch gel was higher than that of the CS-90 starch gel in the higher shear rate region, which was mainly due to the higher content of long chain branches in the CS-90 sample. In the high shear rate region, long chain branches (DP $\geq$ 25) promote chain unfolding and orientation, and the resulting structures are more sensitive to shear and exhibit strong non-Newtonian flow behavior (shear-thinning behavior) (Liu et al., 2021).

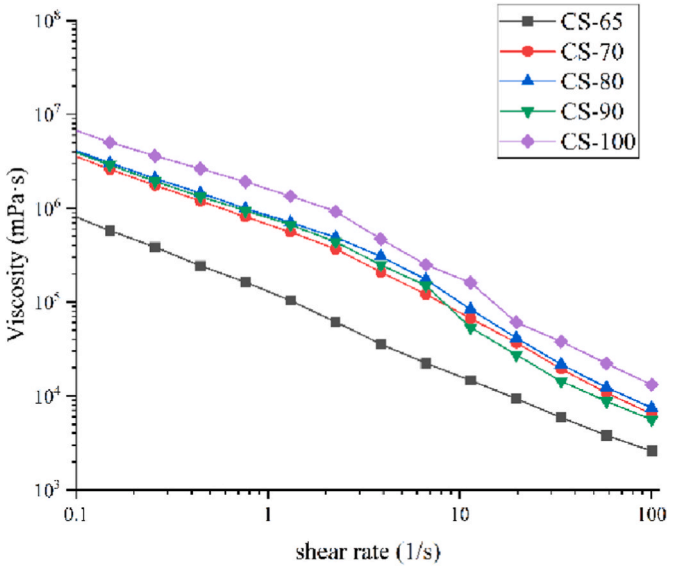

Fig. 4. Viscosity versus shear rate profile of corn starch treated at different temperatures.

3.5.2. Frequency sweep

In the self-supporting stage of 3D printing, the material itself needs to have sufficient structural strength to maintain the stability of the structure, and G′ has an important influence on this stage (Cui et al., 2021a, 2021b). G′ can reflect the structural strength of the material itself to a certain extent. Generally, materials with sufficient structural strength will show better self-supporting performance. G′, expressed as elastic-like solid behavior, is the energy stored during dynamic oscillations. G″ represents the energy dissipated and is related to viscous or liquid-like behavior. As shown in Fig. 5, at the same frequency, the G′ of all samples was larger than G″, indicating the elastic behavior of starch gel samples, which is beneficial for shape stability after 3D printing (Phuhongsung, Zhang, & Bhandari, 2020). With the increase in treatment temperature from 65 to 100 °C, the G′ of the starch gels first increased and then decreased and reached a maximum at a treatment temperature of 80 °C, indicating that a stronger network structure is formed at this temperature, exhibiting stronger solid-like behavior. The increase in the G′ value was mainly attributed to leaching of a higher amylose content, which contributed to a higher level of gelation, thereby increasing the gel strength (Muscat, Adhikari, Adhikari, & Chaudhary, 2012; Zhong et al., 2022). Moreover, the formation of new crystal structures for starch gels treated at higher temperatures also helps to

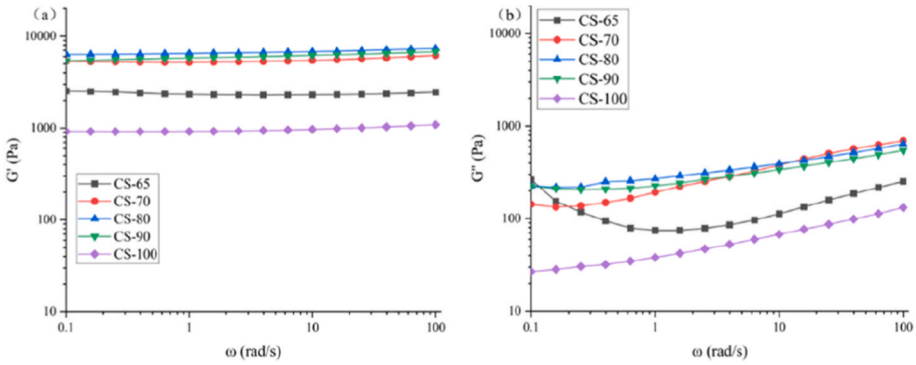

Fig. 5. Storage modulus and loss modulus of corn starch gels treated at different temperatures.

improve the structural strength of starch gel systems (Zeng et al., 2021). On the other hand, the increase in treatment temperature also increased the content of short chain branches (DP 6–12) in the starch gel, which inhibited the interaction between the main chains, resulting in fewer connections in the network structure and a lower G′ value (Liu et al., 2021).

3.5.3. Stress sweep rheological study

Flow stress (τf) refers to the stress value of G' = G″ during the stress scanning process, which is used to characterize the force required to make the material flow and can be also used to reflect the difficulty of extruding the material during extrusion 3D printing. Fig. 6 shows the change in stress sweep for starch samples of different treatment temperatures. When the strain is 1–20 Pa, the G′ and G″ values of the CS slurry basically do not change with the strain, indicating that the CS slurry is in the linear viscoelastic region, and its network structure undergoes reversible deformation without damage. When the strain is greater than 20.8 Pa, the G′ value of the CS-65 sample greatly decreases, while the G″ value increases, and the intersection of G′ and G″ appears at a strain of 65 Pa. This result indicates that the network connection of the CS-65 starch gel samples is dynamically changing in the transition region. With increasing strain, the main chain of starch unfolds, while part of the long branch chain is entangled under shearing. At this point, both the creation and loss rates of connections are positive, resulting in a state of equilibrium where the creation rate is less than the loss rate, resulting in weakened chain tangles. This further disrupts the cohesion of the network structure, leading to the emergence of yield points. The τf of samples increased with increasing temperature from 60 to 80 °C, indicating that CS-65 starch gel samples flow out more easily. The τf values of CS-100 and CS-90 were higher than 1000 Pa. These results showed that starch gels with higher temperature treatment exhibited lower extrudability. The abovementioned results may be explained by the fact that the increase in τf of the starch gels obtained at higher temperatures was attributed to the decrease in long branch chains (DP > 12) and the increase in short chains (DP 6–12), which contributes to the densification of the starch gel structure (Mario et al., 2018). This dense structure results in the incompressibility of the material when subjected to force. In contrast, the starch structures with longer starch chains (DP > 12) have greater steric hindrance, causing them to be more easily compressed when stressed and reaching the τf point more easily.

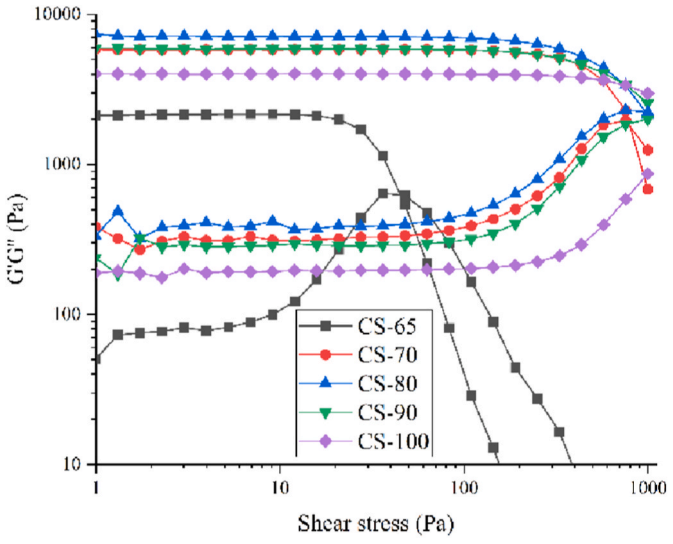

Fig. 6. Stress sweeps for different treatment temperatures of corn starch gels.

3.5.4. Thixotropic test

The material will be subjected to different degrees of shear force during the extrusion 3D printing process. When it is in the storage cylinder, it is subjected to low shear force, and when it passes through the nozzle, it undergoes a high shear process. For extrusion 3D printed materials, it is not only required to be easily extruded from the nozzle under high shear but also to maintain sufficient mechanical integrity after extrusion. That is, the printing material needs to have fast response characteristics to shear strain to ensure that the material, extruded from the nozzle, can quickly recover to a certain structural strength. Therefore, it is very meaningful to explore the response characteristics of the viscosity of starch systems to shear stress for characterizing the thixotropic properties of each starch sample. The thixotropy test can obtain information on the damage and recovery degree of the internal structure of the starch sample under the action of low shear or high shear.

All starch gel systems exhibit a significant decrease in the η value under high strain and rapid recovery under low strain (Fig. 7a), indicating that these starch gel systems have fast response characteristics to strain changes. According to the theory of polymer conformational change, this phenomenon can be seen as a self-healing property of the physical cross-links of the network structure. The decrease in the η value under high shear strain is due to the orientation of the flexible starch macromolecular chains along the shear direction, which leads to a decrease in the conformational entropy of the paste system. The molecular conformation is partially or completely restored, resulting in a gradual recovery of the η value. With increasing temperature, the shear recovery rate of starch gel showed a trend of first increasing and then decreasing (Fig. 7b), and there was a maximum value at the treatment temperature of 80 °C. The increase in the shear recovery rate is due to the leaching of amylose in the starch gel system due to high temperature, which can form more hydrogen bonds with other starch chains and promote the reconstruction process of the shear-damaged starch gel microstructure. The FTIR results also supported the abovementioned analysis. The decrease in shear recovery was attributable to the higher short amylose content, which inhibited the interaction between the main chains, and there were fewer connections in the network structure. In particular, although the CS-100 sample exhibited the highest viscosity

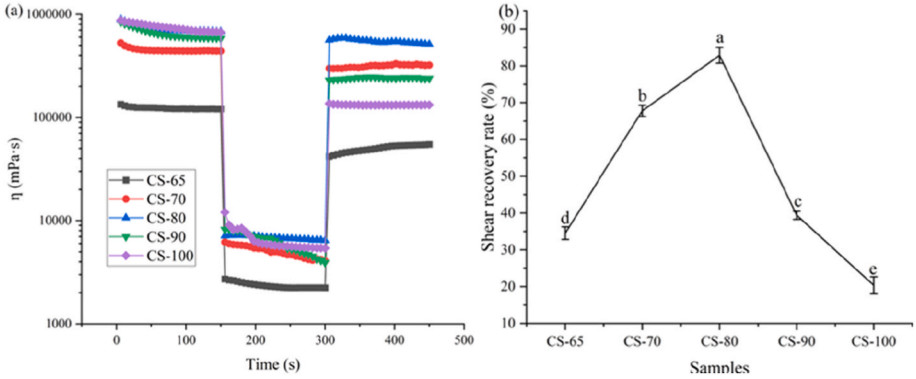

Fig. 7. Alternate strain sweep tests showing η at different temperatures in response to high (100%) and low (1%) oscillatory strains (a) and shear recovery rates (b) for different treatment temperatures of corn starch gels.

before shearing, the CS-80 sample exhibited the highest viscosity after being subjected to high shear, which is beneficial to the structural stability after extrusion (Liu, Bhesh, Sangeeta, Sylvester, & Min, 2018).

3.6. Printability

The corn starch gels were extruded for 3D printing, and the line width and number of layers (Table 2) was related with printing precision and structural strength, respectively (Chen, Xie, Chen, & Zheng, 2018). After the starch material was extruded and printed by a nozzle with a diameter of 0.84 mm, the wire width was significantly larger than 0.84 mm, indicating the occurrence of the extrusion swelling phenomenon. When the viscoelastic material was extruded through a small diameter nozzle, the wire size was significantly affected. Generally, the smaller is the wire width, the smoother and denser is the wire surface, and the higher is the resolution of the printed physical model. With increasing processing temperature (from 65 to 100 °C), the line width of starch gradually decreased, indicating that higher temperature may improve the printing precision of starch gels. The number of printed layers first increases and then decreases with increasing temperature. When the printing temperature is 80 °C, the number of printed layers is the largest. With the increase of the processing temperature, the storage modulus and τf of the starch material continue to increase, and the mechanical properties continue to increase. Therefore, the material can withstand more printing layers without collapse and deformation. When the temperature is 80 °C, the number of printing layers of starch material can reach approximately 56 layers. However, the large flow stress may cause the material to not be ejected from the nozzle smoothly, reducing the continuity of the printing system and reducing the number of printing layers.

As shown in Fig. 8, the samples printed by CS-80 gel was closed to the set model. The CS-65 gel printed sample collapsed and showed an extremely irregular shape, indicating poor printing performance. The edges of the products printed by CS-70 gel were not clear, and the lines cross each other. This was attributed the wider lines of starch gels, which reduced printing accuracy. Compered to CS-70 gel, CS -80, CS-90 and CS-100 gels showed the shape of more rectangular printed product. However, the edges appeared some small bumps and wrinkles for CS-90 and CS-100 gels. This was due to the higher flow stress, starch gels were difficult to be extruded from the plugging nozzle, resulting in discontinuous printing that reduced the fidelity of the printed object.

Table 2
Line width and number of printing layers of corn starch gels treated at different temperatures.

Sample	Line width(mm)	Number of printing layers
CS-65	1.91 ± 0.04a	24±2d
CS-70	1.42 ± 0.06b	41±1b
CS-80	1.05 ± 0.03c	56±1a
CS-90	0.85 ± 0.02d	43±2b
CS-100	0.91 ± 0.05d	35±2c

Different lowercase letters within the same column indicate significant differences between the samples ($p < 0.05$).

3.7. Starch molecular structural contributions to rheological properties and printability

The changes in starch structure under different treatment temperatures are shown in Fig. 9. Thus, the effect of the chain structure caused by the starch treatment temperature on the rheological properties and printability of starch materials can be elaborated. Comparing changes in rheological properties and starch structure, it was clear that the starch chain structure significantly affects the crystal content and network structure of starch gels, which is important for the viscosity and structural strength of the starch gel system (Zeng et al., 2021).

Although the starch particle residue still retains some original crystalline properties (such as CS-65 and CS-70), it has a limited impact on structural strength. Because most of the starch molecular chains of the macromolecular network are confined in the granules, it is difficult to form a denser starch gel network. As previously studied, interactions within free starch chains in gelling systems cause extensive cross-linking, which is important for the formation of tight network structures (Chen et al., 2019). With the increase in the treatment temperature, the amylose is slowly leached out, and the starch chains are extensively cross-linked, forming a cross-linked network structure, which is beneficial to the enhancement of mechanical properties and viscosity. Meanwhile, amylose and lipids form new crystal structures, which improve mechanical properties (Zeng et al., 2021). On the other hand, higher temperature increases the content of short amylopectin (DP 6–12), which increases the density of the starch microstructure and its τf, making it difficult for it to flow and extrude. Ji et al. (2022) also reported that the long amylopectin chains (DP 36–100) was able to increase the hardness of the gels, but this was not conducive to material fluidity during 3D printing. On the other hands, Yi, Zhu, Bao, Quan, and Yang (2020) reported that the decrease of amylopectin chains for $13 < X \leq 24$ induced the springiness of fresh rice noodles. In this study, this was confirmed by CS gel samples treatment temperature from 65 °C to 80 °C. Meanwhile, short amylopectin chains at higher temperature had high mobility, which may destroy the interaction between long starch chains, resulting in unstable gel network structure and weakened structural strength. Therefore, compared with CS-80 gel sample, CS-90 and CS-100 gel samples exhibited lower G′ and print layers.

4. Conclusion

This study reveals the influence of the changes in the molecular

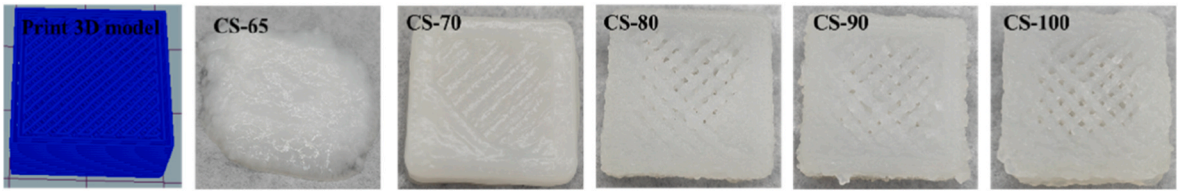

Fig. 8. The microscopic image of printed thread and 3D-printed cuboid for different treating temperatures of corn starch.

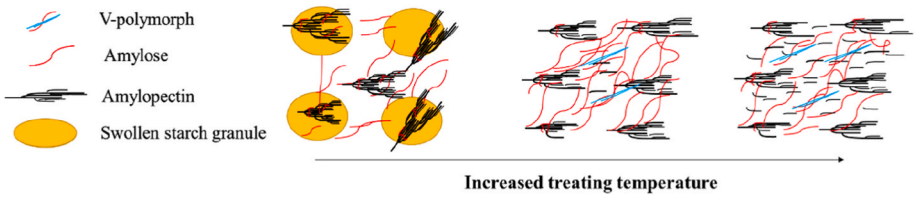

Fig. 9. Schematic diagram of the starch structure changes at different treatment temperatures.

structure of starch caused by treatment temperature on the rheological properties and printability of starch gels. It was observed that with increasing treatment temperature, the leached amylose content and short linear chains (DP 6–12) of corn starch increased, whereas the contents of long linear chains (DP > 12) of amylopectin decreased. Due to the presence of the original granules and crystalline structure, the CS-65 starch gel presented a poor G′. The leaching of amylose promotes the formation of new crystals in starch gels, which is helpful in G′. As the treatment temperature increased, the viscosity and τf of the starch gel samples increased, which was not conducive to extrusion during the 3D printing process. The starch gel samples exhibited the highest G′, shear recovery rate, number of printed layers and printing precision when treated at 80 °C. Enhanced treatment temperature can promote gelatinization of starch and release amylose chains to form gels, whereas temperatures that are too high reduce the effective interaction of starch chains due to the production of short amylopectin. In conclusion, this work provides important information for 3D printing to design personalized high-quality starch-based foods. In the future, the relationship between starch chain structure and its 3D printing properties can be further clarified.

Author statement

Yue Cheng: Methodology, Validation, Formal analysis, Investigation, Data curation, Writing – original draft, Visualization, Kexin, Liang: Investigation, Data curation, Yifan, Chen: Data curation, Wei Gao: Validation, Visualization, Xuemin Kang: Software, Tianze Li: Formal analysis, Bo Cui: Supervision, Funding acquisition, Project administration, Resources, Writing- Review & Editing.

Declaration of interest statement

No.

Data availability

Data will be made available on request.

Acknowledgments

National Key Research & Development Program in China (2019YFD1002704); Key Research and Development Program of Shandong Province (2021CXGC010808, 2021CXGC010807, 2019JZZY010722); the Innovation Team of Jinan City (2018GXRC004); Special Funds for Taishan Scholars Project (NO.ts201712060); Special Project of International Cooperative Research (QLUTGJH2018016); Shandong Bohai Sea Granary Science and Technology Demonstration Project (2019BHLC002); Innovation Pilot Project of Integration of Science, Education and Industry of Shandong Province (2020KJC-ZD011).

Appendix A. Supplementary data

Supplementary data to this article can be found online at https://doi.org/10.1016/j.foodhyd.2022.108364.

References

Ai, Y., & Jane, J. L. (2015). Gelatinization and rheological properties of starch. *Starch Staerke, 67*, 213–224.
Cai, L. A., Goh, K., Lim, K., & Matia-Merino, L. (2021). Rheological characterization of a physically-modified waxy potato starch: Investigation of its shear-thickening mechanism. *Food Hydrocolloids, 120*(6), Article 106908.
Cheng, Y., Gao, S., Wang, W., Hou, H., & Lim, L. (2022). Low temperature extrusion blown ε-polylysine hydrochloride-loaded starch/gelatin edible antimicrobial films. *Carbohydrate Polymers*, (15), Article 118990.
Chen, H., Xie, F., Chen, L., & Zheng, B. (2018). Effect of rheological properties of potato, rice and corn starches on their hot-extrusion 3d printing behaviors. *Journal of Food Engineering, 244*, 150–158.
Chen, Y., Zhang, M., Sun, Y., & Phuhongsung, P. (2021). Improving 3d/4d printing characteristics of natural food gels by novel additives: A review. *Food Hydrocolloids*, (9), Article 107160.
Cheng, Y., Zhai, X., Wu, Y., Li, C., Zhang, R., Sun, C., et al. (2023). Effects of natural wax types on the physicochemical properties of starch/gelatin edible films fabricated by extrusion blowing. *Food Chemistry, 401*, 134081.
Cui, Y., Li, C., Guo, Y., Liu, X., & Yang, F. (2021a). Rheological & 3d printing properties of potato starch composite gels. *Journal of Food Engineering, 313*, Article 110756.
Cui, Y., Li, C., Guo, Y., Liu, X., & Yang, F. (2021b). Rheological & 3d printing properties of potato starch composite gels. *Journal of Food Engineering, 313*(1), Article 110756.
Dankar, I., Haddarah, A., Omar, F., Sepulcre, F., & Pujolà, M. (2018). 3d printing technology: The new era for food customization and elaboration. *Trends in Food Science & Technology*, 231–242, 2018.
Gao, W., Zhu, J., Kang, X., Wang, B., Liu, P., Cui, B., et al. (2021). Development and characterization of starch films prepared by extrusion blowing: The synergistic plasticizing effect of water and glycerol. *LWT–Food Science and Technology, 148*, Article 111820.
Godoi, F. C., Prakash, S., & Bhandari, B. R. (2016). 3d printing technologies applied for food design: Status and prospects. *Journal of Food Engineering, 179*, 44–54.
Hanashiro, I., Abe, J. I., & Hizukuri, S. (1996). A periodic distribution of the chain length of amylopectin as revealed by high-performance anion-exchange chromatography. *Carbohydrate Research, 283*, 151–159.
Huang, S., Chao, C., Yu, J., Copeland, L., & Wang, S. (2021). New insight into starch retrogradation: The effect of short-range molecular order in gelatinized starch. *Food Hydrocolloids, 120*, Article 106921.
Ji, S., Xu, T., Li, Y., Li, H., Zhong, Y., & Lu, B. (2022). Effect of starch molecular structure on precision and texture properties of 3D printed products. *Food Hydrocolloids, 125*, Article 107387.
Kang, X., Liu, P., Gao, W., Wu, Z., Yu, B., Wang, R., et al. (2020). Preparation of starch-lipid complex by ultrasonication and its film forming capacity. *Food Hydrocolloids, 99*, Article 105340.
Li, C., & Hu, Y. (2021). Effects of acid hydrolysis on the evolution of starch fine molecular structures and gelatinization properties. *Food Chemistry, 353*, Article 129449.

Liu, Z., Bhesh, B., Sangeeta, P., Sylvester, M., & Min, Z. (2018). Linking rheology and printability of a multicomponent gel system of carrageenan-xanthan-starch in extrusion based additive manufacturing. *Food Hydrocolloids, 87*, 413–424.

Liu, Z., Chen, L., Bie, P., Xie, F., & Zheng, B. (2021). An insight into the structural evolution of waxy maize starch chains during growth based on nonlinear rheology. *Food Hydrocolloids, 116*, Article 106655.

Li, C., Wu, A., Yu, W., Hu, Y., Li, E., Zhang, C., et al. (2020). Parameterizing starch chain-length distributions for structure-property relations. *Carbohydrate Polymers, 241*, Article 116390.

Lu, H., Tian, Y., & Ma, R. (2023). Assessment of order of helical structures of retrograded starch by Raman spectroscopy. *Food Hydrocolloids, 134*, Article 108064.

Madhusudhan, B., & Tharanathan, R. N. (1996). Structural studies of linear and branched fractions of chickpea and finger millet starches. *Carbohydrate Research, 284*(1), 101–109.

Mario, M., Martinez, C., Li, et al. (2018). Slowly digestible starch in fully gelatinized material is structurally driven by molecular size and A and B1 chain lengths. *Carbohydrate Polymers, 197*, 531–539.

Muscat, D., Adhikari, B., Adhikari, R., & Chaudhary, D. (2012). Comparative study of film forming behaviour of low and high amylose starches using glycerol and xylitol as plasticizers. *Journal of Food Engineering, 109*, 189–201.

Phuhongsung, P., Zhang, M., & Bhandari, B. (2020). 4d printing of products based on soy protein isolate via microwave heating for flavor development. *Food Research International, 137*, Article 109605.

Tang, J., Zou, F., Guo, L., Wang, N., Zhang, H., Cui, B., et al. (2022). The relationship between linear chain length distributions of amylopectin and the functional properties of the debranched starch-based films. *Carbohydrate Polymers, 279*, Article 119012.

Wang, B., Gao, W., Kang, X., Dong, Y., El-Aty, A., & Cui, B. (2021). Structural changes in corn starch granules treated at different temperatures. *Food Hydrocolloids, 118*, Article 106760.

Wang, Q., Li, L., Liu, C., & Zheng, X. (2022). Heat-moisture modified blue wheat starch: Physicochemical properties modulated by its multi-scale structure. *Food Chemistry, 386*, Article 132771.

Wee, M., Matia-Merino, L., & Goh, K. (2015). Time- and shear history-dependence of the rheological properties of a water-soluble extract from the fronds of the black tree fern, cyathea medullaris. *Journal of Rheology, 59*(2), 365–376.

Yin, X., Zheng, Y., Kong, X., Cao, S., Chen, S., & Tian, J. (2021). RG- I pectin affects the physicochemical properties and digestibility of potato starch. *Food Hydrocolloids, 117*, Article 106687.

Yi, C., Zhu, H., Bao, J., Quan, K., & Yang, R. (2020). The texture of fresh rice noodles as affected by the physicochemical properties and starch fine structure of aged paddy. *LWT–Food Science and Technology, 130*, Article 109610.

Zeng, X., Chen, H., Chen, L., & Zheng, B. (2021). Insights into the relationship between structure and rheological properties of starch gels in hot-extrusion 3D printing. *Food Chemistry, 342*, Article 128362.

Zhang, Y., Li, Y., Cai, T., Ahmad, L., Zhang, Y., Qiu, Y., et al. (2022). Hot extrusion 3D printing technologies based on starchy food: A review. *Carbohydrate Polymers, 2022*, Article 119763.

Zhang, Z., Li, E., Fan, X., Yang, C., Ma, H., & Gilbert, R. G. (2020). The effects of the chain-length distributions of starch molecules on rheological and thermal properties of wheat flour paste. *Food Hydrocolloids, 101*, Article 105563.

Zhong, Y., Qu, J., Li, Z., Tian, Y., Zhu, F., & Liu, X. (2022). Rice starch multi-level structure and functional relationships. *Carbohydrate Polymers, 275*, Article 118777.